International Journal of GEOMATE, Aug., 2016, Vol. 11, Issue 24, pp.2241-2247
Geotec., Const. Mat. & Env., ISSN: 2186-2982(Print), 2186-2990(Online), Japan

ESTIMATION OF PERMEABILITY OF POROUS MEDIA WITH MIXED WETTABILITIES USING PORE-NETWORK MODEL

Junichiro Takeuchi, Wataru Sumii, Hidetaka Tsuji and Masayuki Fujihara

Graduate School of Agriculture, Kyoto University, Japan

ABSTRACT: Water flow through porous media is involved with physical factors such as size and configuration of pores, contact angle of grain surface, and connectivity of pores. To deal with these factors, pore-scale modeling is essential. Pore aggregate referred to as pore-network is extracted from randomly packed spherical grains with the modified Delaunay tessellation method. Water flow in a pore-network is formulated in terms of a network flow problem in hydraulics, in which friction and local losses such as contraction and enlargement of pipes are explicitly treated, while those are implicitly included in the hydraulic conductance of capillary tubes in existing works. Through the numerical experiments, it was confirmed that the effect of the local loss on the hydraulic conductivity could be negligible. Furthermore, the relative permeabilities of porous media with mixed wettabilities along the primary drainage and imbibition processes were estimated.

Keywords: Relative Permeability, Network Flow, Friction Loss, Local Loss

1. INTRODUCTION

The constitutive relationship, which is a set of relationships between capillary pressure and saturation, and capillary pressure and relative permeability, is essential for simulations of variously saturated seepage flows. Some functional models such as the van Genuchten model [1] for saturation and the Mualem model [2] for relative permeability are generally utilized in many works. However, since these functional models describe REV (representative element volume)-scale relationships, they cannot treat entrapped air and residual water in pores dynamically. The approaches that enable to deal with interface between water and air are divided into two main groups: one is a continuum-based two-phase flow model and the other is a discrete model which tracks movement, generation, and disappearance of interfaces. The former solves the equations for the mass and momentum conservations numerically in a porous space [3], and the latter simulates water and air intrusion in bond-percolation and invasion-percolation manners in a pore-network [4]. In this study, the latter approach is used since required computational load is relatively small. Another reason for usage of the pore-network approach is hydrophobic grains in a porous medium. It is well known that hydrophobic grains change the hydraulic properties such as water retention characteristics and permeability drastically [5], and the altered hydraulic properties are beyond an applicable scope of the functional models.

In the framework of pore-network model, permeability of an objective medium is estimated on the basis of a flow in pore segments. The flow rate in a pore segment is described by a proportional relation to hydraulic gradient between the ends of a segment. It is the hydraulic conductance that is used as a proportionality coefficient between the flow rate and the hydraulic gradient. Some works derive the conductance from mathematical or numerical analysis of a cross-section, in which the segment is assumed as a pipe with a constant cross-section [6]-[8]. Another derive it from longitudinal or 3-D analysis of a segment, in which a shape of the cross-section varies along the flow path [9], [10]. From a standpoint of hydraulics, the total head loss, which corresponds to the difference of piezometric heads in the segment ends, is described as the summation of the friction loss and local losses such as the enlargement, contraction, entrance, exit, and turning losses, and the equation does not show a linear relationship between the head loss and the flow rate. By the transformation of the equation for the flow rate, it is proved that the conductance derived from the cross-sectional analysis is related to the friction loss when the flow is laminar (APPENDIX). Furthermore, in a case of the conductance derived from the longitudinal or 3-D analysis, the relation between the flow rate and the hydraulic gradient should not be represented linearly in a strict sense, because it contains enlargement and/or contraction losses. Then another question arises: if the relation between the flow rate and the pressure gradient could not be described as a linear equation, why is the Darcy's law represented as a linear equation? In the presented study, an equations system for the pore-network flow is reconstructed in terms of a network flow problem in hydraulics, and the effect of local losses on the hydraulic conductivity is investigated through numerical experiments. And the constitutive relationship between the matric potential and the relative permeability, and the saturation and the relative permeability of porous media mixed with hydrophobic grains at various fractions are estimated.

2. MODEL DESCRIPTION

2.1 Generation of Pore-Network Model

In this study, a virtual pore-networks is extracted from randomly packed spherical grains like glass beads, which are computed with the discrete element method (DEM). From the computed porous media, pore bodies which are relatively large voids and pore throats which are relatively small voids connecting pore bodies are extracted by the modified Delaunay-tessellation approach proposed by Al-Raoush et. al. [11]. In the extraction process, location and size of pore bodies and throats are identified based on the 3-D coordinates of grains. A pore body is represented as an inscribed sphere in the void surrounded by grains, and a pore throat as a cylindrical tube in this study. When the cross-section of a pore throat is represented by a circle, there are three representative circles, (1) the inscribed circle in the void surrounded by grains, (2) the equivalent circle whose area is equal to that of the void, and (3) the effective circle whose hydraulic conductance is equal to that of the void [6] as illustrated in Fig. 1. In some works, the effective radius is given as the arithmetic mean of the inscribed and equivalent radii based on the mathematical and numerical analyses [6], [12], but it might be underestimated since they analyzed the minimum cross-section along the pore throat. In alternate cross-sections other than minimum one, the hydraulic conductivity becomes larger due to the presence of slip walls. Hence, the effective radius is treated as a fitting parameter in this study. Figure 2 shows a computed porous medium with about 58 hundreds uniform spherical grains 0.2 mm in diameter and an extracted pore-network, which consists of 14,522 pore bodies and 36,761 pore throats. The histograms of pore sizes in the pore-network is shown in Fig. 3.

2.2 Formulation Based on Network Flow

In advance to calculation of porous network flow, connected pore-networks whose pore bodies and throats are filled with water are computed in an invasion percolation manner under various conditions relevant to initial states, imposed pressures on the bottom, and mixture fractions of hydrophilic and hydrophobic grains. The detail of the processes is described in the work by Takeuchi et al. [13]. Using the water-filled pore-networks, which are sub-networks of the original pore-network, hydraulic conductivity of each sub-network is calculated under the condition where same pressure is imposed on the top and bottom

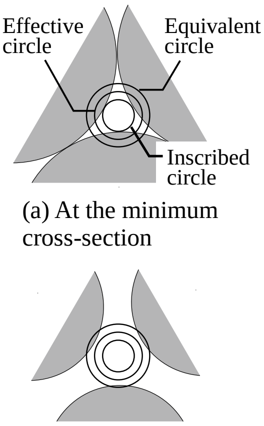

(a) At the minimum cross-section

(b) At alternate cross-section

Fig. 1 Representative circles for a pore throat

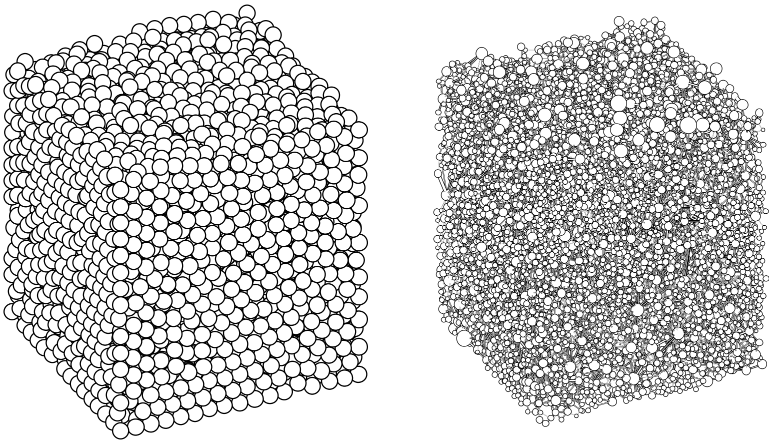

(a) Porous medium model

(b) Pore-network model

Fig. 2 Extraction of pore-network

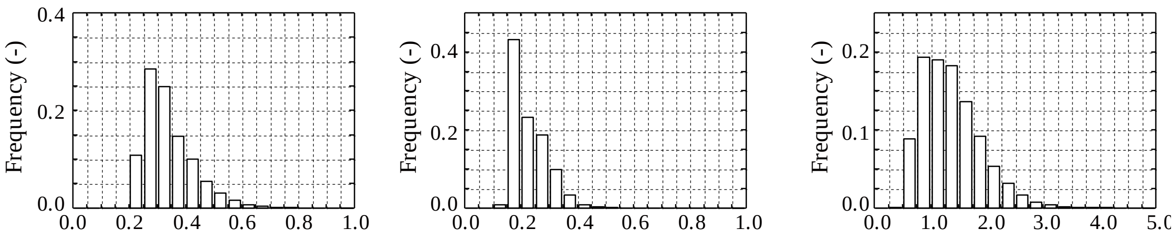

(a) Pore body radius (0.1 mm) (b) Pore throat radius (0.1 mm) (c) Pore throat length (0.1 mm

Fig. 3 Histograms of pore sizes of extracted pore-network model faces of the sub-network. The interfaces between air and water in pores are fixed at the computed location.

Water flow in pore-networks is calculated based on the pipe network analysis, in which local head losses such as enlargement and contraction are considered. In a network flow problem, flow rates in each pipe segment (pore throat and a part of each pore body in this case) and piezometric head at each junction (the center of pore body) are unknown. For simplicity, a segment is represented as a pipe whose cross-section is abruptly contracted and enlarged in this study, and the segment is divided into three parts as illustrated in Fig. 4. Then the total head loss along the segment is described by the empirical equations as follows [14].

$$h_i - h_j = \kappa_k \left| q_k \right| q_k \tag{1}$$

with

$$h_m = \frac{p_m}{\rho g} + z_m \qquad (m = i, j) \tag{2}$$

$$\kappa_k = \left(\sum_{m=i,j,k} \frac{f_m l_m}{2g d_m A_m^2} + \frac{k_S}{2g a_k^2} + \frac{k_E}{2g a_k^2} \right) \tag{3}$$

$$d_m = \frac{4a_m}{P_m} \qquad (m = i, j, k) \tag{4}$$

$$l_i + l_k + l_j = l_{ij} \tag{5}$$

where h_i is the piezometric head at the center of the pore body i, κ_k is the coefficient that includes friction and local losses, f_m is the friction factor, k_S and k_E are the loss coefficients for sudden contraction and sudden enlargement, respectively, l_m is the length of the part m ($m = i, j, k$), d_m is the hydraulic diameter, a_m is the cross-sectional area, q_k is the flow rate in the pore throat k (the segment ij), g is the gravitational acceleration, p_m is the pressure, z_m is the height from a datum, ρ is the water density, P_m is the wetted perimeter, and l_{ij} is the length of the segment ij. When the flow in the pipe is laminar, the friction factor is represented as

$$f_m = \frac{\alpha}{\mathrm{Re}_m} \tag{6}$$

with

$$\mathrm{Re}_m = \frac{\rho d_m \left| q_k \right|}{\mu a_m} \tag{7}$$

where α is a constant that depends on the shape of the cross-section and its value is 64, 56.908, and 53.333 for the circular, square, and equilateral-triangular cross-section, respectively [15]; Re_m is the Reynolds number; and μ is the water viscosity. Equations (6) and (7) indicate that the coefficient κ_k depends on the flow rate q_k, that is $\kappa_k = \kappa_k(q_k)$.

The mass balance at each junction (pore body here) except for inflow and outflow pore bodies is described as follows.

$$\sum_{k \in \eta_i} q_k = 0 \tag{8}$$

where η_i is the set of pore throats connecting the pore body i.

In addition to Eqs. (1) and (8), the piezometric heads in the inflow and outflow pore bodies, into or from which water flows freely depending on the prescribed head, are given as follows.

$$h_m = h_m^* \qquad (m \in \eta^{\mathrm{IN}}, \eta^{\mathrm{OUT}}) \tag{9}$$

where η^{IN} and η^{OUT} are the sets of the inflow and outflow pore bodies, respectively.

The network flow problem in a pore space, which is described by Eqs. (1) through (9), is a non-linear equations system, and it is solved by the Newton method. The coefficient $\kappa_k(q_k)$ is estimated from the previous q_k in the iterative process of the Newton method in the same way with a linearization technique for the Richards equation [16], and when the flow rates in some pores are zero or extremely small, a sufficiently small value (e.g., 10^{-20}) is given to q_k since q_k is included in denominator (Eqs. (6), and (7)) in this study to avoid crashes in computing.

When the local losses (sudden contraction and enlargement losses here) are negligible compared with the friction loss, Eq. (1) becomes the conductance-based equation, which is generally used in different works (e.g., [6]-[10]), and described as follows (APPENDIX).

$$h_i - h_i = \frac{l_{ij}}{\rho g \Theta_{ij}} q_k \tag{10}$$

where Θ_{ij} is the hydraulic conductance between the nodes i and j. Then the equations system becomes linear.

The above mentioned formulation indicates that the hydraulic conductance Θ_{ij} is related to the friction losses and the shape of the cross-section, and it does not include other local losses. Furthermore, it implies that the conductance derived from longitudinal or 3-D analysis should not be used, since it contains some local effects like contraction, enlargement, and turning losses. If these effects are considered, the equation relating to the flow rate and head loss (the pressure difference) becomes non-linear as shown by Eqs. (1) through (7).

The hydraulic conductivity of the sub-network, which is the unsaturated one, is estimated based on the Darcy's law.

$$K = \frac{QL}{A \Delta H} \tag{11}$$

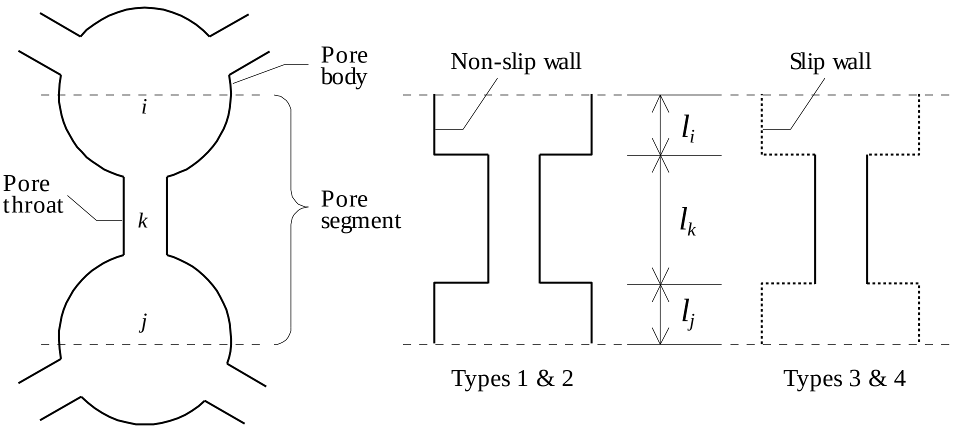

Fig. 4 Configurations of pore segment

with

$$Q = \sum_{k \in \eta_{PT}^{IN}} q_k = \sum_{k \in \eta_{PT}^{OUT}} q_k \tag{12}$$

where K is the hydraulic conductivity of variously saturated porous media, Q is the total flow rate through the medium, η_{PT}^{IN} and η_{PT}^{OUT} are the sets of the pore throats connecting to the inflow and outflow pore bodies, L and A are the length and the cross-sectional area of the medium, and ΔH is the difference of the piezometric head between the inflow and outflow faces. The saturated hydraulic conductivity K_S is computed from the pore-network in which all the pore bodies and pore throats are filled with water, and the relative permeability K_r is obtained by the following relation.

$$K_r = \frac{K}{K_S} \tag{13}$$

3. NUMERICAL EXPERIMENTS

3.1 Configuration of Pore Segments

Firstly, an effect of configuration of pore segments between pore bodies on the hydraulic conductivity is investigated. In this study, four types of segment, which are designed to consider how the pore bodies are dealt, are tested (Fig. 4). In the all types, pore bodies on both ends are treated as relatively large circular tubes, and a pore throat as a relatively narrow circular tube. In Type 1, the friction losses of both large and narrow tubes and the local losses for sudden contraction and enlargement are considered, while only friction losses are considered in Type 2. In Types 3 and 4, the large tubes are assumed to have slip walls. Type 3 has the local losses for sudden contraction and enlargement, and Type 4 does not have such local losses.

The saturated hydraulic conductivities of the extracted pore-network (Fig. 1) are computed, as the lengths of the large-tubes vary from 0 to 0.04 mm. The tube with a constant cross-section ($l_i = l_j = 0$) is treated as a standard, and the effective radius r^{eff} of tubes is adjusted based on the inscribed radius r^{ins}, i.e., $r^{eff} = \omega r^{ins}$, where ω is a coefficient, in order that the hydraulic conductivity becomes about 2×10^{-2} cm/s. For the objective pore-network the value of the coefficient is identified as 1.38, and the hydraulic conductivity is reproduced as 2.006×10^{-2} cm/s. The values of k_S and k_E are given as 0.5 and 1.0, respectively, and each value becomes maximum when the sudden contraction and enlargement are supposed to be the entrance and exit, respectively.

The obtained result is shown in Fig. 5. It is found that all the hydraulic conductivities increase at accelerated paces as the length of large tubes increases, and the increasing pace of Types 3 and 4 is large compared with Types 1 and 2. This

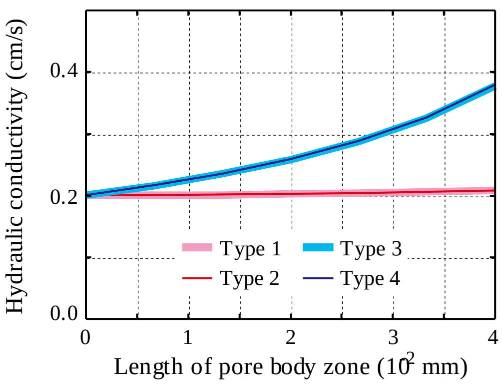

Fig. 5 Relation of hydraulic conductivity and pore segment configuration

indicates that the friction losses in pore bodies need to be introduced, but the effect is limited. Furthermore, it is shown that the effects of the local losses are negligible. Actually, the ratio of the local losses and the friction loss in a typical segment ($r^{ins} = 0.03$ mm, $l_k = 0.1$ mm) is about 6 $\times 10^{-3}$ if the Reynolds number is 0.17, which is a half of the maximum Reynolds number.

3.2 Relative Permeability

To calculate the relative permeability of variously saturated pore-networks, various states

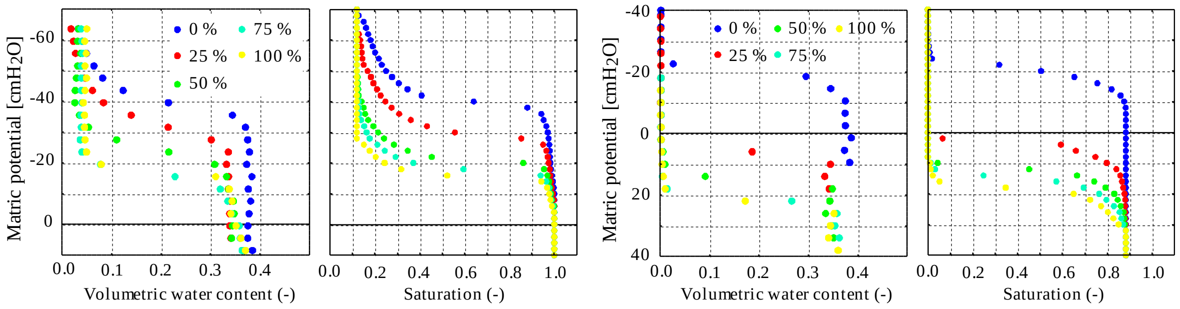

(a) Measurement (b) Computation (a) Measurement (b) Computation

6-1 Drainage process 6-2 Imbibition process

Fig. 6 Measured and computed water retention curves of porous media with mixed wettabilities

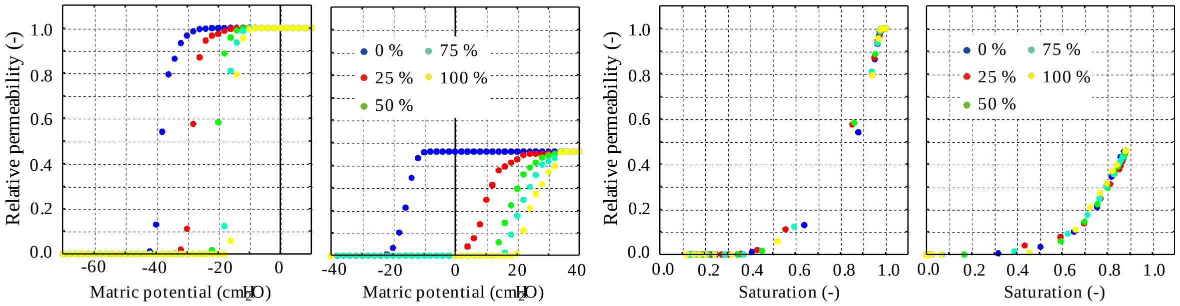

(a) Drainage process (b) Imbibition process (a) Drainage process (b) Imbibition process

7-1 Relative permeability vs. matric potential 7-2 Relative permeability vs. saturation

Fig. 7 Relative permeability in drainage and imbibition processes

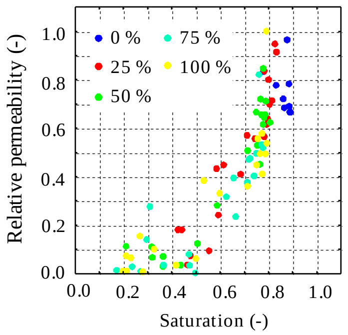

Fig. 8 Measured relative permeability

along drainage and imbibition processes are needed. Then, water retention curves for the primary drainage and the primary imbibition of the extracted pore-network are computed in an invasion percolation manner, which is the same way with our previous work [13]. The objective porous media are presumed to include hydrophilic and hydrophobic grains in various proportions. The mixture fraction of hydrophobic grains ranges from 0% to 100% at 25% interval. The contact angles of the hydrophilic and hydrophobic grains, which are essential factors that determines the water retention properties, are identified by a trial-and-error adjustment so as to fit the observed results. The identified values are listed in Table 1, where different values are given to the contact angles for the drainage and imbibition processes. These are considered to correspond to the receding and advancing contact angles. Besides, in the drainage or imbibition process different values are given to hydrophilic grains even in accordance with the mixture fraction. It is considered that the hydrophilic (original) glass beads are partially hydrophobized by the redundant coating material (octyltrichlorosilane, OTS) that remains on the hydrophobized grain surfaces. This speculation is consistent with our experiments on measurements of the water drop penetration time, the apparent contact angle, and the water-entry pressure [17]. The computed and measured water retention curves are shown in Fig. 6.

At each point along the primary drainage and imbibition processes, sub-networks in which pores are filled with water are withdrawn, and the hydraulic conductivity is computed if the sub-network stretches out from the bottom up to the top. Here, the constant-radius tubes without sudden contraction and enlargement ($l_i = l_j = 0$, and $\omega = 1.38$) are used. Common pressure head is imposed to the pore bodies on the bottom and top

Table 1 Contact angles (deg)

process	mixture fraction	hydrophilic grain	hydrophobic grain
drainage	0%	46	74
	25%	50	
	50, 75, 100%	60	
imbibition	0%	58	110
	25%	92	
	50, 75, 100%	98	

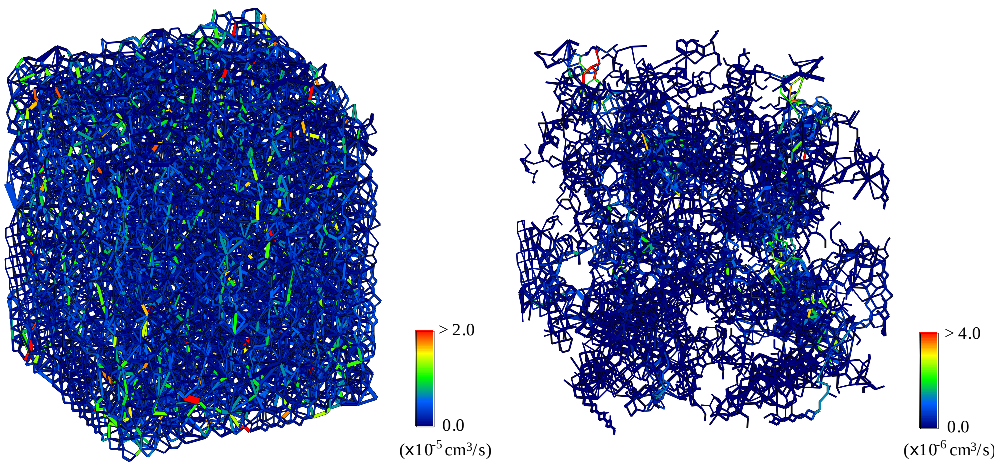

(a) 0%, -22 cmH_2O (b) 50%, -22 cmH_2O

Fig. 9 Flow distributions in various mixture fractions (drainage process)

faces, then the hydraulic gradient becomes unit. Therefore, water flows down by the gravity through the porous medium.

Figure 7-1 shows the relation of the relative permeability and the matric potential in the drainage and imbibition processes. This figure corresponds to the water retention curves in Fig. 6. Figure 7-2 shows the computed relation of the relative permeability and the saturation, and it indicates similar tendency with measured one (Fig. 8). The measured one was obtained with the constant head method (Daiki, DIK-4012). Although the method is normally used for measurement of the saturated hydraulic conductivity, variously saturated glass beads of diameter 0.1 mm with mixed wettabilities are used in this study.

Figure 9 shows some typical flow distributions in pore-networks. These figures indicate water flows in only a minority of pores especially in unsaturated states since many terminals are included in the pore-network.

4. CONCLUSION

Water flow through porous media is re-formulated in terms of a network flow problem in hydraulics, where friction and local losses such as sudden contraction and enlargement are incorporated. The equations system becomes nonlinear in contradiction to the Darcy's law, which expresses a linear relation between flow rate and hydraulic gradient, if the local losses are introduced. Through the numerical experiments with a virtual pore-network extracted from randomly packed spherical grains, it is confirmed that the system could be regarded as a linear system because the local losses are negligible compared with the friction loss. Furthermore, relative permeabilities of porous media with mixed wettabilities along primary drainage and imbibition processes are estimated, and the results indicated a similar tendency with the measured one.

5. APPENDIX

When the local losses are negligible compared with the friction loss, Eq. (1), which stands for total loss in the segment between the nodes i and j becomes as follows.

$$h_i - h_j = \left(\sum_{p=i,j,k} \frac{l_p}{\rho g \Theta_p} \right) q_k \tag{14}$$

with

$$\Theta_p = \frac{2 d_p^2 A_p}{\alpha \mu} \tag{15}$$

When the harmonic average is taken between the nodes i and j, the hydraulic conductance Θ_{ij} of the segment becomes as follows.

$$\frac{l_{ij}}{\Theta_{ij}} = \frac{l_i}{\Theta_i} + \frac{l_k}{\Theta_k} + \frac{l_j}{\Theta_j} \tag{16}$$

Then, the flow rate q_k is represented as follows.

$$q_k = \Theta_{ij} \frac{\rho g \left(h_i - h_j \right)}{l_{ij}} \tag{17}$$

6. ACKNOWLEDGEMENT

This work was supported by JSPS KAKENHI Grant Number 24780232.

7. REFERENCES

[1] van Genuchten MT, "A closed form equation for predicting the hydraulic conductivity of unsaturated soils", Soil Sci. Soc. Am. J., Vol. 44, 1980, pp. 892-898.

[2] Mualem Y, “A new model for predicting the hydraulic conductivity of unsaturated porous media”, Water Resour. Res., Vol. 12, 1976, pp. 513-522.
[3] Ferrari A, Jimenez-Martines J, Borgne TL, Mehuest Y, and Lanati I, “Challenges in modeling unstable two-phase flow expriments in porous micromodels”, Water Resour. Res., Vol. 51, 2015, doi:10.1002/201WR016384.
[4] Gharbi O, Blunt MJ, “The impact of wettability and connectivity on relative permeability in carbonates: a pore network modeling analysis”, Water Resour. Res., Vol. 48, 2012, doi:10.1029/2012WR011877.
[5] DeBano LF, “Water repellency in soils: a historical overview”, J. Hydrol., Vol. 231-232, 2000, pp. 4-32.
[6] Bryant S and Blunt M, “Prediction of relative permeability in simple porous media”, Phys. Rev. A, Vol. 46, 1992, pp. 2001-2011.
[7] Patzek TW and Silin DB, “Shape factor and hydraulic conductance in noncircular capillaries I. One-phase creeping flow”, J. Colloid Interface Sci., Vol. 236, 2001, pp. 295-304.
[8] Valvatne PH and Blunt MJ, “Predictive pore-scale modeling of two-phase flow in mixed wet media”, Water Resour. Res., Vol. 40, 2004, doi:10:1029/2003WR002627.
[9] Koplik J, “Creeping flow in two-dimensional networks”, J. Fluid Mech., Vol. 119, 1982, pp. 219-247.
[10] Dagan Z, Weinbaum S, and Pfeffer R, “An infinite-series solution for the creeping motion through an orifice of finite length”, J. Fluid Mech., Vol. 115, 1982, pp. 505-523.
[11] Al-Raoush R, Thompson K, and Willson CS, “Comparison of network generation technique for unconsolidated porous media”, Soil Sci. Soc. Am. J., Vol. 67, 2003, pp. 1687-1700.
[12] Bryant S, King PR, and Mellor DW, “Network model evaluation of permeability and spatial correlation in a real random sphere packing”, Trans. Porous Media, Vol. 11, 1993, pp.53-70.
[13] Takeuchi J, Sumii W, and Fujihara M, “Modeling of fluid intrusion into porous media with mixed wettabilities using pore network”, in Proc. 5th Int. Conf. on GEOMATE, 2015, pp. 748-754.
[14] Larock BE, Jeppson RW, and Watters GZ, Hydraulics of Pipeline Systems, CRC Press, 2000, p. 537.
[15] Shah RK, “Laminar flow friction and forced convection heat transfer in duct of arbitrary geometry”, Int. J. Heat Mass Transfer, Vol. 18, 1975, pp. 849-862.
[16] Huyakorn PS and Pinder GF, Computational Methods in Subsurface Flow, Academic Press, 1983, p.473.
[17] Takahashi T, Hydraulic properties of porous media with mixed wettabilities, Graduation Thesis of Kyoto University, 2013, p.45 (in Japanese).

International Journal of GEOMATE, Aug., 2016, Vol. 11, Issue 24, pp. 2241-2247.
MS No. 5127j received on July 30, 2015 and reviewed under GEOMATE publication policies.

Corresponding Author: Junichiro Takeuchi